Magnetoacoustic Relaxation by Cr²⁺ Jahn–Teller Centers Revealed from Elastic Moduli

Vladimir V. Gudkov,* Isaac B. Bersuker, Irina V. Zhevstovskikh, Maksim N. Sarychev, Sergei Zherlitsyn, Shadi Yasin, and Yuri V. Korostelin

Magnetoacoustic investigations of the ZnSe:Cr²⁺ crystal with sphalerite structure, performed in Faraday geometry, show that there is a new channel of relaxation by the Cr²⁺ Jahn–Teller (JT) centers, induced by the magnetic field. A new method is worked out that allows to extract the relaxation time, either from the temperature changes of the elastic modulus in fixed magnetic field or from the magnetic field dependences at fixed temperatures. Application of both approaches to the imaginary part of the elastic modulus prove their efficiency and indicate that the magnetic field-dependent relaxation rate reaches the magnitude of about $10^6 \, \mathrm{s}^{-1}$ at $T = 1.3 \, \mathrm{K}$.

1. Introduction

Among diluted magnetic semiconductors bivalent chromium centers represent particular interest due to their specific properties. Recently a first-principle study of the Cr²⁺-doped ZnSe has been published.[1] Experimental studies revealed a ferromagnetic *p-d* exchange in the valence band (in contrast to Mn, Co, and Fe centers, which exhibit antiferromagnetic exchange[2]), and a large spin to strain coupling.[3] The latter makes Cr very promising as a spin qubit for the realization of hybrid spin-mechanical systems, in which the motion of a microscopic mechanical oscillator would be coherently coupled to the spin state of a single atom.[4] As in the majority of systems with open-shell impurities, ZnSe:Cr²⁺ is subject to the Jahn–Teller effect (JTE) with specific local properties.[5]

The ultrasonic technique provides a unique opportunity for the study of impurities in solids. Typically ultrasound experiments deal with temperature dependences of the phase velocity or attenuation. But in view of possible application in quantum computing,[3,6] magneto-acoustic investigation is deemed to be important. We have performed such experiments in wurtzite CdSe:Cr²⁺,[7] fluorite SrF₂:Cr²⁺,[8] and sphalerite ZnSe:Cr²⁺[9] single crystals. All of these materials manifest the JTE but only ZnSe:Cr²⁺[10] exhibits magnetic field dependence of the acoustic properties. In the ZnSe matrix, Cr²⁺ substitutes zinc in tetrahedral coordination and forms the JT complexes CrSe₄ with the chromium ion in the electronic ground state $^5T_2$ (e^2t^2) in the high spin configuration, subject to the $T \otimes e$ JTE problem.[5,9] Its adiabatic potential-energy surface (APES) represents three paraboloids, which are equivalent in the absence of external perturbations, but become non-equivalent under the ultrasound, following its wave of deformations (see **Figure 1**).

Initial experiments[10] carried out at 24 MHz resulted in the discovery of a peak in magnetic field dependencies of the ultrasonic attenuation at 2 K. At first, the peak was interpreted as due to a resonance, but the results obtained later revealed that it is likely to be of relaxation origin. This was confirmed by the attenuation measurements versus temperature in fixed magnetic fields. A shape variation was observed for the attenuation maximum,[11] which definitely had its relaxation origin in zero fields.

In the theory of elasticity, the tensor of elastic moduli **c** describes the stiffness of the crystal and enters the stress-and-strain relation. The process of energy dissipation, which characterizes the wave propagation, involves the effective moduli as complex variables: $c_{\mathrm{m}} = \omega^2 \kappa_{\mathrm{m}}^{-2} \rho$, where c_{m} is a linear combination of the tensor components defined in the Cartesian system. It determines the complex wave-number $\kappa_{\mathrm{m}} = k_{\mathrm{m}} - i a_{\mathrm{m}}$ of the normal mode m with the real part $k_{\mathrm{m}} = \omega / v_{\mathrm{m}}$ and imaginary one written as $-a_{\mathrm{m}}$, where v_{m} is the phase velocity, a_{m}

Prof. V. V. Gudkov, Dr. I. V. Zhevstovskikh, M. N. Sarychev
Institute of Physics and Technology
Ural Federal University
19, Mira st., Ekaterinburg 620002, Russia
E-mail: gudkov@imp.uran.ru

Prof. I. B. Bersuker
Institute for Theoretical Chemistry
the University of Texas at Austin
Austin, TX 78712, USA

Dr. I. V. Zhevstovskikh
M. N. Miheev Institute of Metal Physics
UB, RAS, 18, S. Kovalevskaya st., Ekaterinburg 620137, Russia

Dr. S. Zherlitsyn, Dr. S. Yasin[+]
Hochfeld-Magnetlabor Dresden (HLD-EMFL)
Helmholtz-Zentrum Dresden-Rossendorf
01328 Dresden, Germany

Dr. Yu. V. Korostelin
P. N. Lebedev Physical Institute
RAS, 53, Leninskiy Prospect, Moscow 119991, Russia

The ORCID identification number(s) for the author(s) of this article can be found under https://doi.org/10.1002/pssa.201800586.

[+]Present address: College of Engineering and Technology, American University of Middle East, Egaila 54200, Kuwait

ADVANCED
SCIENCE NEWS

www.advancedsciencenews.com

physica
status
solidi
pss
a

www.pss-a.com

Figure 1. The adiabatic potential energy surface of Cr^{2+} centers in ZnSe: Cr^{2+}, subject to the $T \otimes e$ problem of the JTE, consists of three equivalent paraboloids (filled surfaces). The contour plots schematically show the shifts initiated by the ultrasonic wave.

is the attenuation coefficient, ρ is the mass density of a crystal, and ω is cyclic frequency of the ultrasonic wave. For small variations of the variables and for positive k_m we have

$$\frac{\Delta c_m}{c_0} = -2\left(\frac{\Delta k_m}{k_0} - i\frac{\Delta a_m}{k_0}\right) \tag{1}$$

where the symbol Δ indicates the difference of the variable with respect to its reference value, i.e., $\Delta c_m = c_m(A) - c_m(A_0)$, $c_0 = c_m(A_0)$, A is an external parameter (temperature, magnetic field, etc.), A_0 is a reference value, and $k_0 = \omega/v_m(A_0)$. At zero field ($\mathbf{B} = 0$) the JT subsystem contributes to the total elastic modulus[12]

$$\frac{c_{JT}}{c_0} = -\frac{\left(c_{JT}^S - c_{JT}^T\right)}{c_0}\frac{1 - i\omega\tau}{1 + (\omega\tau)^2} \tag{2}$$

where τ denotes the time of relaxation to the equilibrium distribution of the states localized in minima of the APES, shifted by the strains induced by the ultrasonic wave (see Figure 1). c_{JT}^S and c_{JT}^T are the adiabatic and isothermal contributions of the JT subsystem to the total elastic modulus. The adiabatic modulus c_{JT}^S vanishes because the impurities remain in thermal equilibrium with the environment (for more details see page 136 in ref. [12]). In our case of the wavevector $\boldsymbol{\kappa} \parallel [110]$ and polarization $\mathbf{u} \parallel [1\bar{1}0]$, the tetragonal-symmetry moduli c_m, c_{JT}, c_0, c_{JT}^S, and c_{JT}^T, with $c_E = (c_{11} - c_{12})/2$, which allow us, for simplicity, to omit the subscript E in Equation (2), as well as in further consideration.

In addition to our previous investigations of the ZnSe:Cr^{2+} crystal (construction of the APES based on the temperature dependences of attenuation,[9] discovery of the magnetic field dependence of attenuation,[10] and observation and interpretation of the variation of the relaxation peak of attenuation on its temperature dependence approximately at $T = 11$ K in fixed magnetic fields), and in *further development of the trend as a whole*, we report here a novel approach to study relaxations in JT centers in crystals: using a new technique, we extract the magnetic field dependence of the relaxation time from the imaginary part of the elastic modulus obtained from the ultrasound experiments, as described below in this paper. Added to the earlier worked out methodology of ultrasound investigation of impurity crystals, the new approach contributes significantly to its accuracy and reliability.

2. Experimental Section

The experiments were carried out at the Dresden High Magnetic Field Laboratory using setup operating as a frequency variable bridge.[13] The setup for the ultrasonic measurements shown in **Figure 2** is based on a pulse-echo method and phase-sensitive detection technique. High-frequency mechanical oscillations in the piezoelectric transducer 1 were excited by a radio pulse with duration of about 1 μs. After propagation through the sample, the oscillations were transformed into an electric signal by another piezoelectric transducer 2 located on the opposite side of the sample. Received radio pulses were amplified and mixed with two phase-shifted reference signals of the same frequency. After suppressing the second harmonic with low-pass filters and integrating the resulting signals with gated box-car averagers, the output dc signal, Q, was used for the frequency modulation, keeping the phase constant and providing information about the sound-velocity changes. Another dc signal, I, is related to the ultrasound attenuation. More details are given in ref. [14]. The measurements were carried out at $\omega/2\pi = 33.1$ MHz in a

Figure 2. Simplified diagram of the setup used for ultrasonic investigation. Abbreviation used here are RF, radio frequency; FM, frequency modulation.

longitudinal magnetic field, meaning the vector of magnetic induction **B** was parallel to the wave vector $\boldsymbol{\kappa}$. The sample of perfect quality has dimensions of $4 \times 5 \times 5$ mm^3. It was cut from a single crystal manufactured at the P.N. Lebedev Physical Institute of the Russian Academy of Sciences. The zinc selenide crystal was grown in a quartz ampoule by physical vapor transport technique in a helium atmosphere onto the ZnSe seed[15] with the CrSe source for doping.

The magnetic field dependence of ImΔc at several temperatures is shown in **Figure 3**. An increase of Im$\Delta c(T)$ has been detected at low temperatures when the magnetic field was applied (**Figure 4**).

3. Magnetic Field-Dependent Relaxation Time

To describe the results shown in Figure 3 and 4, we use Equation (2) with the modulus $c_{\text{JT}}^{\text{T,B}}$ and relaxation time $\tau(T, B)$ defined at fixed magnetic field. We assume that the magnetic field induces a new channel of relaxation (similar to ref. [16]). It means that the relaxation rate should be written as follows

$$\tau(T, B)^{-1} \equiv \tau_{\text{T,B}}^{-1} = \tau_{\text{T}}^{-1} + \tau_{\text{B}}^{-1} \tag{3}$$

where τ_{B} is the part of relaxation time induced by the magnetic field only, and τ_{T} is the temperature-dependent relaxation time defined at $B = 0$. The τ_{T} value was derived for the impurity zinc selenide crystal in ref. [17]. The relaxation contribution of the impurity subsystem: $c_{\text{JT}}(T)/c_0 = (c(T) - c_{\text{b}}(T))/c_0$, where $c(T)$ is the total dynamic modulus, and $c_{\text{b}}(T)$ is a background modulus determined by all the other contributions of the crystal. According to Equation (2), Im(c_{JT}/c_0) vanishes at $T \to 0$ and $T \to \infty$, so Im$c_{\text{b}}(T)$ can be approximated by a monotonic function which coincides with Im$c(T)$ at low and high temperatures. In our case we consider the high temperature regime established at $T = 30$ K, and assume that

$$\text{Im}\Delta c_{\text{b}}(T) = -4.47 \cdot 10^{-4} + 8.35 \cdot 10^{-5} \cdot T^{0.4}$$
$$+ \frac{1.17 \cdot 10^{-3}}{(3.2 \cdot T - 0.17)^{0.4}} - 2.61 \cdot 10^{-6} \cdot T \tag{4}$$

which includes the mentioned above constraints on Imc_{JT}. The relaxation time at $B = 0$ can be defined as follows

$$\tau_{\text{T}} = \frac{1}{\omega} \left\{ \frac{\text{Im}c_{\text{JT}}(T_1) \cdot T_1}{\text{Im}c_{\text{JT}}(T) \cdot T} \pm \sqrt{\left(\frac{\text{Im}c_{\text{JT}}(T_1) \cdot T_1}{\text{Im}c_{\text{JT}}(T) \cdot T} \right)^2 - 1} \right\} \tag{5}$$

where T_1 corresponds to the condition $\omega\tau(T_1) = 1$. The upper sign in Equation (5) is taken for $T \geq T_1$, while the lower one relates to $T < T_1$. The isothermal modulus is $c_{\text{JT}}^{\text{T}} \propto 1/T$,[12] so we can rewrite Equation (2) for Imc_{JT} in the form

$$\text{Im}\frac{c_{\text{JT}}}{c_0} = 2\text{Im}\frac{c_{\text{JT}}(T_1) \cdot T_1}{c_0 T} \left[\frac{\omega\tau}{1 + (\omega\tau)^2} \right] \tag{6}$$

As mentioned above, the analysis of the elastic modulus in magnetic fields should be carried out with the substitution of c_{JT}^{T} by $c_{\text{JT}}^{\text{T,B}}$, and $\tau(T)$ by $\tau(T, B)$. The first substitution is realized by means of a pre-factor β $\left(c_{\text{JT}}^{\text{T,B}} = \beta c_{\text{JT}}^{\text{T}} \right)$, and for the second one, according to Equation (3), we have

$$\text{Im}\frac{c_{\text{JT}}(T, B)}{c_0} = 2\beta \frac{\text{Im}c_{\text{JT}}(T_1) \cdot T_1}{c_0 T} \frac{\omega\left(\tau_{\text{T}}^{-1} + \tau_{\text{B}}^{-1}\right)^{-1}}{1 + \left[\omega\left(\tau_{\text{T}}^{-1} + \tau_{\text{B}}^{-1}\right)^{-1} \right]^2} \tag{7}$$

For comparison with the experimental curve we should evaluate the total modulus using Equations (7) and (4), as follows

$$\text{Im}\frac{\Delta c(T, B)}{c_0} = \text{Im}\frac{c_{\text{JT}}(T, B)}{c_0} + \text{Im}\frac{\Delta c_{\text{b}}(T)}{c_0} \tag{8}$$
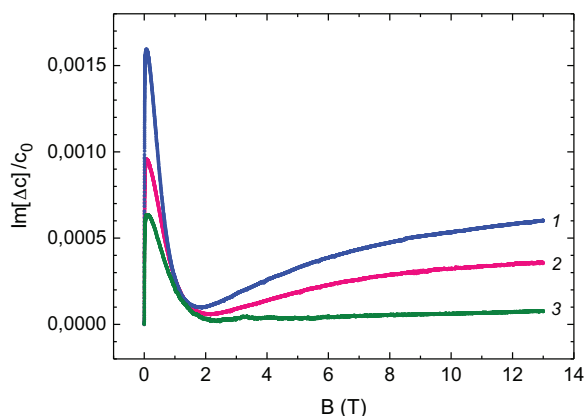

Figure 3. Dependence of the imaginary part of the tetragonal elastic modulus on the magnetic field. Curves 1–3 correspond to $T = 1.3$, 2.5, and 4 K, respectively. $\Delta c = c(\omega, T, B) - c(\omega, T, 0)$.
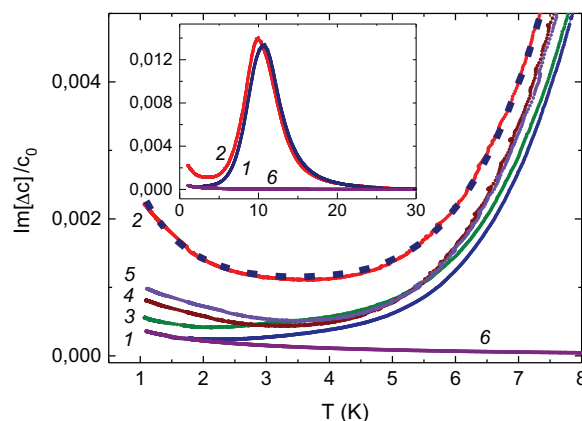

Figure 4. Temperature dependence of the imaginary part of the tetragonal elastic modulus in different magnetic fields. Curves 1–5 correspond to $B = 0$, 0.15, 1.5, 7, and 12 T, respectively. Curve 6 shows the background contribution given by Equation (4). Dashed line 2 is obtained by simulation for $B = 0.15$ T, $\Delta c = c(\omega, T, B) - c(\omega, T_0, B)$, $T_0 = 30$ K.

Table 1. Results of $Im[\Delta c(T, B)/c_0]$ fitting.

B, T	0	0.04	0.15	0.7	1.5	3.6	7	12
τ_B, 10^{-6} s	∞	1	1	2.5	9	10	3.5	2.5
β	1	1.2	1.3	1.1	1.1	1.1	1.1	1.1

An example of such simulation carried out for $B = 0.15\,T$ is shown by the dashed line in Figure 3, and the fitting parameters for all the measured curves are given in **Table 1**.

We can now determine τ_B using the experimental data on the magnetic field dependence of $Im c(T, B)$ at fixed temperatures. The Δc_b value is assumed to be independent of the magnetic field, and the right-hand part of equation $\Delta c(T, B) = c(T, B) - c(T, B = 0)$ is given by Equations (7) and (6)

$$Im\frac{\Delta c(T, B)}{c_0} = Im\frac{c_{JT}(T, B)}{c_0} - Im\frac{c_{JT}(T, B = 0)}{c_0} \quad (9)$$

Keeping in mind that the regime $\omega\tau(T, B) >> 1$ holds below 5 K in applied magnetic field too, we can solve Equation (9) with respect to τ_B^{-1}

$$\tau_B^{-1} = \left\{ \frac{\omega}{2\beta}\frac{Im\Delta c(\omega, T, B) \cdot T}{Im\Delta c_{JT}(\omega, T_1) \cdot T_1} - \frac{(\beta - 1)}{\beta}[\tau_T(T)]^{-1} \right\} \quad (10)$$

The curve $\tau_B^{-1}(B)$ following Equation (10) with an average value of $\beta = 1.2 \pm 0.1$ is shown in Figure 4. Obviously, the assumption that τ_B is a temperature-independent magnetic field induced relaxation time is well supported by the good agreement between the experimental data and the results of simulation (see **Figure 5**). Note also that the obtained numerical values of $\tau_B(B)$, given in Table 1, are quite reasonable.

The interpretation of the experimental function $\tau_B^{-1}(B)$ can be given based on the corresponding dependence of ultrasonic attenuation (or $Im c$) on B, because at $\omega\tau(T, B) >> 1$ the attenuation is proportional to τ^{-1}. In ref. [16], the increase of $\tau_B^{-1}(B)$ with B from 0 to 0.1 T was interpreted as due to a

new channel of relaxation via tunneling from one distorted configuration of the JTE center to another one, made possible by the magnetic field-induced coupling between their otherwise orthogonal orbital states. The decrease from 0.1 to 2 T was explained as due to the change of the attenuation mechanism with the relaxation replaced by quasi-resonance transitions between greatly broadened energy levels, so that only decaying tail-resonance dependence is seen.

A similar procedure for $\tau_B(B)$ evaluation can be developed based on the data on the real part of the elastic modulus. In this case τ_T can be obtained from the following expression[18]

$$\tau_T = \frac{1}{\omega}\left\{ \sqrt{\left(\frac{Re c_{JT}(T_1) \cdot T_1}{Re c_{JT}(T) \cdot T}\right)^2 - 1} \right\} \quad (11)$$

By analogy with Equation (9) we have

$$Re\frac{\Delta c(T, B)}{c_0} = Re\frac{c_{JT}(T, B)}{c_0} - Re\frac{c_{JT}(T, B = 0)}{c_0} \quad (12)$$

This equation is equivalent to

$$Re\frac{\Delta c(T, B)}{c_0} = 2\beta\frac{Re c_{JT}(T_1) \cdot T_1}{c_0 T}\frac{1}{1 + \left[\omega(\tau_T^{-1} + \tau_B^{-1})^{-1}\right]^2}$$
$$- 2\frac{Re c_{JT}(T_1) \cdot T_1}{c_0 T}\frac{1}{1 + [\omega\tau_T]^2} \quad (13)$$

Its solution with respect to τ_B^{-1} yields an expression for calculating the magnetic field-dependent contribution to the relaxation rate, assuming, as above, $\omega\tau(T, B) >> 1$

$$\tau_B^{-1} = \omega\left\{ \frac{1}{2\beta}\frac{Re\Delta c(\omega, T, B) \cdot T}{Re\Delta c_{JT}(\omega, T_1) \cdot T_1} + [\tau_T(T)]^{-2} \right\}^{1/2} - [\tau_T(T)]^{-1} \quad (14)$$

However, this approach based on employing the data on the real part of the moduli encounters a significant difficulty. In contrast to the imaginary contribution $Im c_b$, the real part of the background elastic modulus exhibits temperature variation comparable with the JTE-induced variation $Re c_{JT}(T)$. The background elastic modulus can be approximated by the Varshni formula[19]

$$Re\Delta c_b = -c_0\frac{s}{\exp(\theta/T) - 1} \quad (15)$$

where s and θ are fitting parameters. This approach was reported in ref. [20]. It works well in the vicinity of $T = T_1$. At low temperatures $T \leq 5\,K$ of interest to our problem the accuracy of τ_T determination by this method proved to be unsatisfactory.

4. Conclusion

i) Magnetoacoustic investigation of the ZnSe:Cr^{2+} crystal has been performed at low temperatures in applied magnetic fields; ii) the analysis of the results shows that anomalies in temperature and magnetic field dependence of the elastic
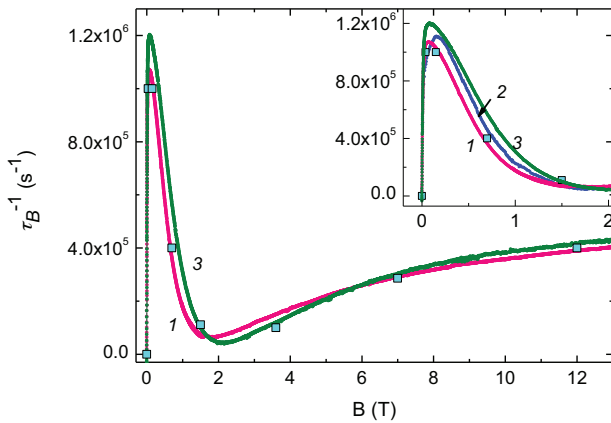

Figure 5. Magnetic field dependence of the relaxation rate τ_B^{-1} calculated after Equation (10), and the experimental data obtained at $T = 1.3\,K$ (curve 1), 2 K (curve 2), and 2.5 K (curve 3). Square symbols are the result of fitting with the parameters given in Table 1.

moduli originate from relaxation in the JT impurity subsystem; iii) for a full interpretation of the experimental results, a new method has been developed allowing to extract the relaxation time in magnetic fields either from the temperature dependence of the elastic modulus in fixed magnetic fields or from magnetic field dependence at fixed temperatures; iv) this method can be effectively used in experimental data analysis of any similar problem.

Acknowledgments

Conflict of Interest

The authors declare no conflict of interest.

Keywords

[1] Y. Zhang, G. Feng, S. Ning, S. Zhou, *Phys. Status Solidi B* **2016**, *253*, 1133.

[2] W. Mac, A. Twardovski, P. J. T. Eggenkamp, H. J. M. Swagten, Y. Shapira, M. Demianiuk, *Phys. Rev. B* **1994**, *50*, 14144.

[3] A. Lafuente-Sampietro, H. Utsumi, H. Boukari, S. Kuroda, L. Besombes, *Appl. Phys. Lett.* **2016**, *109*, 053103.

[4] P. Rabl, S. J. Kolkowitz, F. H. L. Koppens, J. G. E. Harris, P. Zoller, M. D. Lukin, *Nat. Phys.* **2010**, *6*, 602.

[5] I. B. Bersuker, *The Jahn-Teller Effect*. Cambridge University Press, Cambridge, UK **2006**.

[6] M. Mehring, *Phys. Status Solidi B* **2007**, *244*, 3868.

[7] N. S. Averkiev, I. B. Bersuker, V. V. Gudkov, I. V. Zhevstovskikh, M. N. Sarychev, S. Zherlitsyn, Sh. Yasin, Yu. V. Korostelin, *J. Appl. Math. Phys.*, **2017**, *5*, 26.

[8] I. V. Zhevstovskikh, I. B. Bersuker, V. V. Gudkov, N. S. Averkiev, M. N. Sarychev, S. Zherlitsyn, S. Yasin, G. S. Shakurov, V. A. Ulanov, V. T. Surikov, *J. Appl. Phys.* **2016**, *119*, 225108.

[9] V. V. Gudkov, I. B. Bersuker, I. V. Zhevstovskikh, Yu. V. Korostelin, A. I. Landman, *J. Phys. Condens. Matter* **2011**, *23*, 115401.

[10] V. V. Gudkov, I. B. Bersuker, S. Yasin, S. Zherlitsyn, I. V. Zhevstovskikh, V. Yu. Mayakin, M. N. Sarychev, A. A. Suvorov, *Solid State Phenom.* **2012**, *190*, 707.

[11] I. V. Zhevstovskikh, V. V. Gudkov, M. N. Sarychev, S. Zherlitsyn, S. Yasin, I. B. Bersuker, N. S. Averkiev, K. A. Baryshnikov, A. M. Monakhov, Yu. V. Korostelin, *Appl. Magn. Reson.* **2016**, *47*, 685.

[12] M. D. Sturge, in *Solid State Physics*, Vol. 20 (Eds: F. Seitz, D. Turnbull, H. Ehrenreich), Academic Press, New York **1967**, p. 92.

[13] S. Zherlitsyn, S. Yasin, J. Wosnitza, A. A. Zvyagin, A. V. Andreev, V. Tsurkan, *Low Temp. Phys.* **2014**, *40*, 123.

[14] B. Wolf, B. Luthi, S. Schmidt, H. Schwenk, M. Sieling, S. Zherlitsyn, I. Kouroudis, *Physica B* **2001**, *294–295*, 612.

[15] Y. V. Korostelin, V. I. Kozlovsky, *J. Alloys Compd.* **2004**, *371*, 25.

[16] N. S. Averkiev, I. B. Bersuker, V. V. Gudkov, I. V. Zhevstovskikh, K. A Baryshnikov, M. N. Sarychev, S. Zherlitsyn, S. Yasin, Yu. V. Korostelin, *Phys. Rev. B* **2017**, *96*, 094431.

[17] V. Gudkov, A. Lonchakov, V. Sokolov, I. Zhevstovskikh, N. Gruzdev, *Phys. Status Solidi B* **2005**, *242*, R30.

[18] V. V. Gudkov, in *The Jahn–Teller Effect* (Eds: H. Koppel, D. R. Yarkony, H. Barentzen), Heidelberg, Dordrecht, London **2009**, p. 743.

[19] Y. P. Varshni, *Phys. Rev. B* **1970**, *2*, 3952.

[20] N. S. Averkiev, I. B. Bersuker, V. V. Gudkov, I. V. Zhevstovskikh, M. N. Sarychev, S. Zherlitsyn, S. Yasin, G. S. Shakurov, V. A. Ulanov, V. T. Surikov, *J. Phys. Soc. Jpn.* **2017**, *86*, 114604.